Relationship between modern rainfall variability, cave dripwater, and stalagmite geochemistry in Guam, USA

Judson W. Partin

Institute for Geophysics, Jackson School of Geosciences, University of Texas at Austin, J. J. Pickle Research Campus, Building 196, 10100 Burnet Road (R2200), Austin, Texas 78758-4445, USA (jpartin@ig.utexas.edu)

John W. Jenson

Water and Environmental Research Institute of the Western Pacific, University of Guam, Mangilao, Guam 96923

Jay L. Banner

Department of Geological Sciences, Jackson School of Geosciences, University of Texas at Austin, 1 University Station C9000, Austin, Texas 78712-0254, USA

Terrence M. Quinn and Frederick W. Taylor

Institute for Geophysics, Jackson School of Geosciences, University of Texas at Austin, J. J. Pickle Research Campus, Building 196, 10100 Burnet Road (R2200), Austin, Texas 78758-4445, USA

Daniel Sinclair

Institute of Marine and Coastal Sciences, Rutgers University, New Brunswick, New Jersey 08901, USA

Benjamin Hardt

Department of Geological Sciences, Jackson School of Geosciences, University of Texas at Austin, 1 University Station C9000, Austin, Texas 78712-0254, USA

Mark A. Lander and Tomoko Bell

Water and Environmental Research Institute of the Western Pacific, University of Guam, Mangilao, Guam 96923

Blaž Miklavič

Water and Environmental Research Institute of the Western Pacific, University of Guam, Mangilao, Guam 96923

Department of Geosciences, Mississippi State University, Starkville, Mississippi 39762, USA

John M. U. Jocson

Water and Environmental Research Institute of the Western Pacific, University of Guam, Mangilao, Guam 96923

Danko Taboroši

Geology Department, American University of Beirut, PO Box 11-0236, Riad El-Solh, Beirut 1107 2020, Lebanon

[1] Modern rainwater, cave dripwater and cave stalagmite geochemical time series from a cave in Guam (13°38′N, 144°53′E) are used to better understand how changes in cave stalagmite geochemistry relate to aboveground changes in rainfall at a tropical location. A scientific field team based in Guam collects ~monthly samples from multiple sites for geochemical analyses at a cave and aboveground rainfall from a nearby location. We compute a transfer function between rainfall amount and oxygen isotopic composition ($\delta^{18}O$) of a decrease (increase) of 0.94 ± 0.3 m/year for every 1‰ increase (decrease) in rainfall $\delta^{18}O$, based on data extracted from the International Atomic Energy Agency (IAEA) Global Networks of Isotopes in Precipitation (GNIP) database and from data generated in this study. Dripwater $\delta^{18}O$ and Mg/Ca ratios show annual cyclicity at some, but not all sites, accentuating the complex nature of cave hydrology. A stalagmite $\delta^{18}O$ record for the last ~160 years indicates the existence of droughts of decadal length, when rainfall is estimated to be ~0.65 ± 0.3 m/year less than average conditions. This estimate of rainfall reduction most likely refers to wet season months, as these months preferentially contribute to groundwater recharge. The proxy-based climate record at Guam provides new evidence highlighting how a rainy site in the Western Pacific Warm Pool today can experience considerable changes in rainfall on decadal timescales.

1. Introduction

[2] The Western Pacific Warm Pool (WPWP) represents a major source of heat and water vapor in the climate system and influences climate across the globe on timescales including annual (wet/dry seasons), interannual (El Niño-Southern Oscillation, ENSO) [*Rasmusson and Wallace*, 1983; *Ropelewski and Halpert*, 1987], and decadal (Pacific Decadal Oscillation, PDO) [*Mantua et al.*, 1997; *Zhang et al.*, 1997]. The WPWP has warmed, freshened, and expanded from 1955 to present, possibly due to anthropogenic forcing [*Cravatte et al.*, 2009]. Proxy records of climate variability (sea surface temperature (SST), sea surface salinity (SSS), rainfall) in the WPWP are needed to extend beyond the instrumental period so that multidecadal scale variability can be placed in broader context [*Quinn et al.*, 1993; *Guilderson and Schrag*, 1999; *Clement et al.*, 2000; *Stott et al.*, 2002; *Rosenthal et al.*, 2003; *Juillet-Leclerc et al.*, 2006; *Quinn et al.*, 2006]. Moreover, forecasts by global climate models (GCM) do not agree on how precipitation in the WPWP will change over the next 100 years, in part due to the paucity of data that hinders the robust assessment of the natural climate variability of this important region [*Cane et al.*, 1997; *Timmermann et al.*, 1999;

Intergovernmental Panel on Climate Change, 2007]. Characterization of natural climate variability preceding the historical record, however, is attainable only by studies of natural climate proxies such as tree rings, lacustrine and marine sediments, corals, and cave deposits. The accuracy and precision of the interpretation of paleoclimate proxies such as cave deposits (or stalagmites), however, is limited by our understanding of the physical and chemical processes that control proxy composition as measured in modern cave studies.

[3] Most modern cave studies are concentrated in the midlatitudes and sub-tropics [*Fairchild et al.*, 2000; *Genty et al.*, 2001; *Cruz et al.*, 2005; *Spotl et al.*, 2005; *Treble et al.*, 2005a; *Banner et al.*, 2007; *Fuller et al.*, 2008; *Lorrey et al.*, 2008; *Bradley et al.*, 2010; *Jex et al.*, 2010; *Boch et al.*, 2011; *Frisia et al.*, 2011; *Schimpf et al.*, 2011]. Studies of cave water isotopic composition from the deep tropics have to date been limited to several cave and rainfall studies [*Banner et al.*, 1996; *Fleitmann et al.*, 2004; *Mickler et al.*, 2004; *Cobb et al.*, 2007] and two rainfall-only studies [*Griffiths et al.*, 2009; *Lachniet*, 2009]. Modern cave studies monitor physical and chemical changes in the cave and assess the correlation between cave processes and environmental changes that occur aboveground (see reviews by *Fairchild*
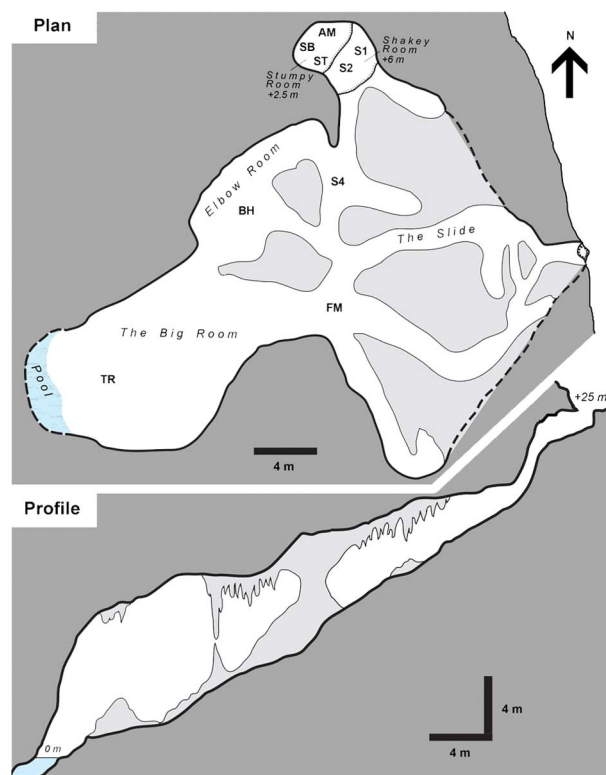
Figure 1. Cave map of Jinapsan Cave, Guam, USA (13.4°N, 144.5°E). The 10 monitored sites are marked: Flatman (FM), Station 4 (S4), Borehole (BH), Station 1 (S1), Station 2 (S2), Stumpy (ST), Stumpy's Brother (SB), Amidala (AM), Trinity (TR), Pool. Cave temperature is relatively constant at ∼26°C and relative humidity is ∼100% year-round providing an ideal setting for paleoclimate studies. Levels provided for Stumpy Room, Shakey Room, and the cave entrance are relative to the level of water in the pool, assumed to be approximate mean sea level.

et al. [2006], *Baker et al.* [2008], and *Fairchild and Treble* [2009]), whereas stalagmite studies provide paleoclimate reconstructions. In the midlatitudes and sub-tropics, a large annual cycle in temperature causes changes in cave atmospheric dynamics, whereas tropical cave systems are simpler in that the temperature and dynamic changes in the cave during the year are minimal. As a result, proxies in tropical caves are thought to respond mostly to changes in precipitation. Similar to modern cave studies, paleoclimate reconstructions using tropical stalagmites are also more limited than those in the midlatitudes, as suitable tropical caves are mostly in relatively remote and inaccessible locations [*Banner et al.*, 1996; *Burns et al.*, 2003; *Partin et al.*, 2007; *Westaway et al.*, 2007; *van Breukelen et al.*, 2008; *Griffiths et al.*, 2009]. Fortunately, systematic exploration and mapping of the karst features of the Mariana Islands during the past decade, led by researchers based at the University

of Guam's Water and Environmental Research Institute of the Western Pacific and Mississippi State University's Department of Geosciences, has revealed a number of caves with promising formations, particularly in Guam [*Taboroši et al.*, 2003; *Jenson et al.*, 2006].

[4] Specifically, this study exploits the ∼monthly monitoring of a tropical cave system initiated in 2008 to compare the observed variations in Guam rainfall with geochemical variations in rainwaters, cave dripwaters, and a stalagmite from Jinapsan Cave, Guam (13°38′N, 144°53′E). This study adds significant new data to quantify past changes in rainfall using cave deposits as proxies, which heretofore has seen only a limited number of studies [*Banner et al.*, 1996; *Fairchild et al.*, 2000; *Fleitmann et al.*, 2004; *Banner et al.*, 2007; *Cobb et al.*, 2007; *Fuller et al.*, 2008; *Mattey et al.*, 2008; *Griffiths et al.*, 2009]. In this paper, we develop a transfer function for the conversion of the stable oxygen isotopic composition (δ^{18}O) in Guam stalagmites to rainfall amount that facilitates the interpretation of past rainfall variations at Guam extending back in time to ∼1840 CE.

2. Methods

2.1. Cave Monitoring

[5] A monthly collection program of cave dripwater was established in August 2008 at ten collection stations in Jinapsan Cave, Guam (Figure 1). A biweekly collection program of integrated samples of rainwater was established in October 2008, following International Atomic Energy Agency (IAEA) protocol. We also analyzed available rainwater data from 1961 to 1978 (111 months with 5 complete climatological (April to March) years intermittent in the range of data) from the IAEA database (Global Network of Isotopes in Precipitation: The GNIP database, International Atomic Energy Agency and World Meteorological Organization, 2006, available at http://www.iaea.org/water) to supply information about interannual changes in the isotopic composition of rainfall. Instrumentation in the cave includes rain gauges that continuously log measurements of drip rates, temperature sensors, relative humidity sensors, and a CO_2 monitor. On-site drip rate is determined by either counting the number of drips per minute if the rate is fast enough or by deploying a pre-weighed bottle to determine the volume of water discharged over time. The stable isotopic composition of rain and cave dripwater was measured on a Thermo Scientific Delta V Isotope Ratio Mass Spectrometer (IRMS) equipped with a

GasBench sample introduction system at the University of Texas at Austin. Analytical precision (2σ) on waters is $\pm8‰$ for deuterium (δD) and $\pm0.2‰$ for oxygen ($\delta^{18}O$). Water isotopic measurements are reported in ‰ VSMOW. Trace metal ratios in cave dripwater were measured using an Inductive Coupled Plasma-Optical Emission Spectrometer (ICP-OES), Perkin-Elmer Optima 4300 DV at the University of Texas at Austin, with a typical analytical precision of 4% for elemental composition and 5% for trace metal ratios (2σ). Rain gauge measurements are from a daily record from Anderson Air Force Base, which is ~8km SE from the cave entrance.

2.2. Paleoclimate Analyses of the Stalagmite "Stumpy"

[6] A subsample of the stalagmite "Stumpy," located 6.3 mm from the top of the stalagmite, was dated using ^{238}U-decay series geochronology and thermal ionization mass spectrometry (TIMS) at the University of Texas at Austin in 2006 (following methods given by *Musgrove et al.* [2001]) to within an error of 13% (2σ). The stalagmite "Stumpy" formed under the drip "Stumpy," which is located in a side chamber of Jinapsan Cave (Figure 1). The stalagmite is 300 mm long and yellowish in color. The upper part of the sample is clearer with some white banding, and the bottom is more opaque with white and brown banding. A 2 mm wide transect at ~6 mm depth in the sample (near the region sampled for U-Th dating) was analyzed using powder X-ray diffraction (XRD). XRD analysis shows a large peak at a 2θ of 29.4°, indicating calcite, and no intensity at the double peaks near 26°, indicating an absence of aragonite. Therefore, the upper 7 mm of the stalagmite is 100% calcite, as this portion is optically homogeneous. Calcite powders from the stalagmite were continuously milled every 150 μm using a computer-controlled drill, and the stable isotopic composition was measured by a Delta V Isotope Ratio Mass Spectrometer (IRMS) with a Kiel Device at the University of Texas at Austin. Analytical precision (2σ) for carbonates is $\pm0.08‰$ for $\delta^{13}C$ and $\pm0.12‰$ for $\delta^{18}O$. Calcite isotopic measurements are reported in ‰ VPDB. Stalagmite trace metal ratios were measured using Laser Ablation-Inductive Coupled Plasma-Mass Spectrometer (LA-ICP-MS) (New Wave/Agilent 7500ce) at the University of Texas at Austin, with a laser spot size of 10 μm, scanning the sample at 5 μm/sec, pulsing the laser at 15 Hz, and software integration times of 0.020 s. Software output data were averaged with a 15-point running mean to produce a final record with resolution of ~5 μm/point (8–10 points/year).

Data were calibrated by measurement of NIST glass standard 610 before and after scans. Additional NIST glass 610 samples were run in between sample paths and were treated as unknowns. Percent recovery for the unknown NIST glass 610s were with 0.2% of accepted values and the standard deviation of the unknowns were <1.3% for Mg and 0.6% for Sr ppm (N = 4). Four paths ~3 mm apart, as well as three scans ~50 μm apart, reproduce the same mean mmol/mol and range of variability of Mg/Ca (~12 $\pm$ 3 mmol/mol) and Sr/Ca (~0.14 $\pm$ 0.04 mmol/mol), however fine-scale variations are not exactly reproduced, most likely due to sub-mm-scale heterogeneity in stalagmite layers (Figure S1 in Text S1 in the auxiliary material).[1] One scan of the six (bottom-most blue scan in Figure S1 in Text S1) was chosen to represent Mg/Ca variability in the stalagmite.

2.3. Estimating Mean Annual $\delta^{18}O$ at Drip Sites

[7] An estimate of the weighted mean annual $\delta^{18}O$ in cave drip water at Station 1 was determined using measured drip rates (in mL/min). In three cases, drip rate measurements were not available because the collection bottle fell over (March 2009), overflowed (October 2009), or the amount collected was low enough that only an estimate could be made (April 2010). To determine the drip rate in mL/min for these three time periods, we relied on drop counts per unit time, which show a linear relationship with drip rates in mL/min (y = 0.071x + 0.0035, R^2 = 0.97). In addition, the $\delta^{18}O$ of drip water from March 2009 was used as an estimate of the March 2010 value. While it is unlikely that drip $\delta^{18}O$ will be exactly equivalent between March of 2009 and 2010, it is a reasonable approximation and helps emphasize the variability in the weighted mean $\delta^{18}O$ due to drip rate and during the other months of the year.

3. Results and Discussion

3.1. Cave Parameters

[8] The environmental conditions in this tropical cave (temperature, relative humidity, air pCO_2, etc.) provide a favorable setting for a stalagmite to faithfully record changes in aboveground rainfall. The mean annual cave air temperature is 26 $\pm$ 0.5°C (Onset Hobo Pro V2 data), and this small amount of annual temperature variability translates to ~0.1‰
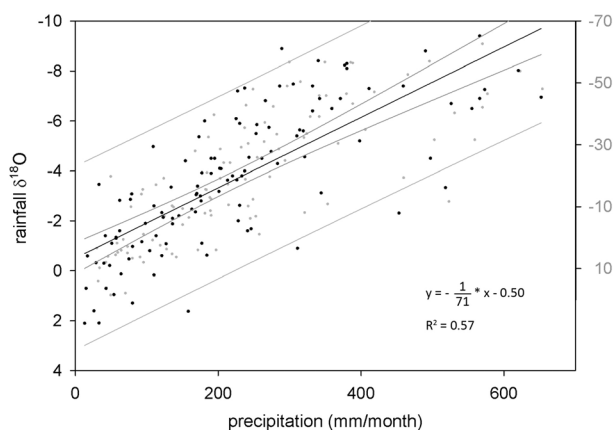

Figure 2. Oxygen and hydrogen isotopic composition of Guam rainfall plotted versus rainfall amount in Guam: $\delta^{18}O$ (black circles) and δD (gray circles). Note both $\delta^{18}O$ and δD are plotted on an inverse scale to match the convention presented in the following figures (higher rainfall upwards). Data are an average of values extracted from the Global Network of Isotopes in Precipitation database (GNIP - http://isohis.iaea.org) and samples collected for this study (∼1961–1978 and 2008–2010, respectively). Empirical inverse relationship between rainfall amount and stable isotopic composition, the so-called "Amount Effect," explains 57% of the variance in rainfall $\delta^{18}O$. Linear fit (95% confidence and prediction bands shown) yields a relationship of ∼71 mm/month of rainfall change for every 1‰ change in rainfall $\delta^{18}O$.

change in calcite $\delta^{18}O$ [*Epstein et al.*, 1953], which is within analytical error of mass spectrometer measurements. Continuous measurements logged using a Vaisala CO_2 probe (Model GMP70) in the side chamber near site S2 (Figure 1) show mean pCO_2 of 1050 ppm (median = 660; max = 6100; min = 84) over a discontinuous period from August 2008-October 2011. Cave air pCO_2 is near or below the 900 ppm threshold calculated by *Buhmann and Dreybrodt* [1985] for most of the year, suggesting minimal biasing in the calcite record of dripwater geochemical composition [*Buhmann and Dreybrodt*, 1985]. Year-round cave air relative humidity of ∼100% (Onset Hobo Pro V2 data) leaves little room for evaporative effects to influence calcite $\delta^{18}O$ [*Hendy*, 1971].

3.2. Rainfall Data

[9] Rainfall in Guam displays a strong annual cycle in both amount and stable isotopic composition ($\delta^{18}O$ and δD); however dry season variability drives interannual variability in all variables. Approximately 60% of the rainfall (∼1500 mm of the 2600 mm annual total) occurs in the rainy season: June to October. On average, Guam rainfall

$\delta^{18}O$ shifts from roughly −8‰ in the wet season to ∼0‰ in the dry season, whereas δD ranges from −45‰ to 0‰ (Figure 2). On interannual time-scales, the $\delta^{18}O$ difference between wet and dry season can range from 6‰ to 12‰ (Figure 2), mostly dependent upon the intensity and duration of the dry season, where wet season values tend to saturate at approximately −8‰.

[10] There is a clear, inverse relationship between rainfall amount in Guam and rainfall $\delta^{18}O$ and δD on both monthly (Figure 2) and yearly (Figures 3a and 3b) timescales. This empirical relationship, known as "the amount effect," is observed across the tropics and sub-tropics [*Dansgaard*, 1964; *Rozanski*
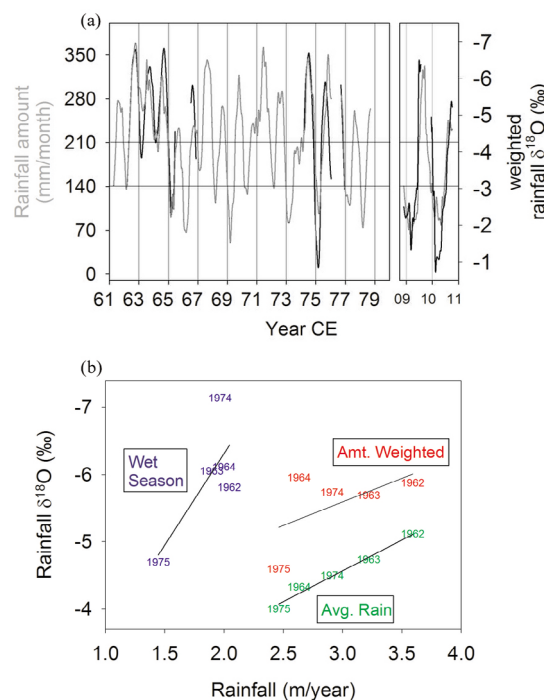

Figure 3. (a) Smoothed rainfall and $\delta^{18}O$ time series at Guam. Rainfall amount data are smoothed with a 7-month running mean. Rainfall $\delta^{18}O$ data are smoothed with a 7-month rainfall amount-weighted running mean to simulate mixing in the overlying bedrock. Rainfall $\delta^{18}O$ faithfully captures both the annual cycle and interannual variability in rainfall amount. The horizontal bars cover a range of 71 mm/month and correspond to a change of ∼1‰ in rainfall $\delta^{18}O$, supporting the relationship calculated in Figure 1. (b) Estimates of annual rainfall $\delta^{18}O$ for 5 complete years (data labels) using three different methods: average rainfall $\delta^{18}O$ (green), amount weighted rainfall $\delta^{18}O$ (red), and wet season only (May–October) rainfall $\delta^{18}O$ (blue) versus the amount of rainfall. While the data is limited (N = 5) and appreciable scatter exists, the relationship of a decrease (increase) of ∼1 m/year for every 1‰ increase (decrease) in rainfall $\delta^{18}O$ holds on interannual timescales using three different methods.
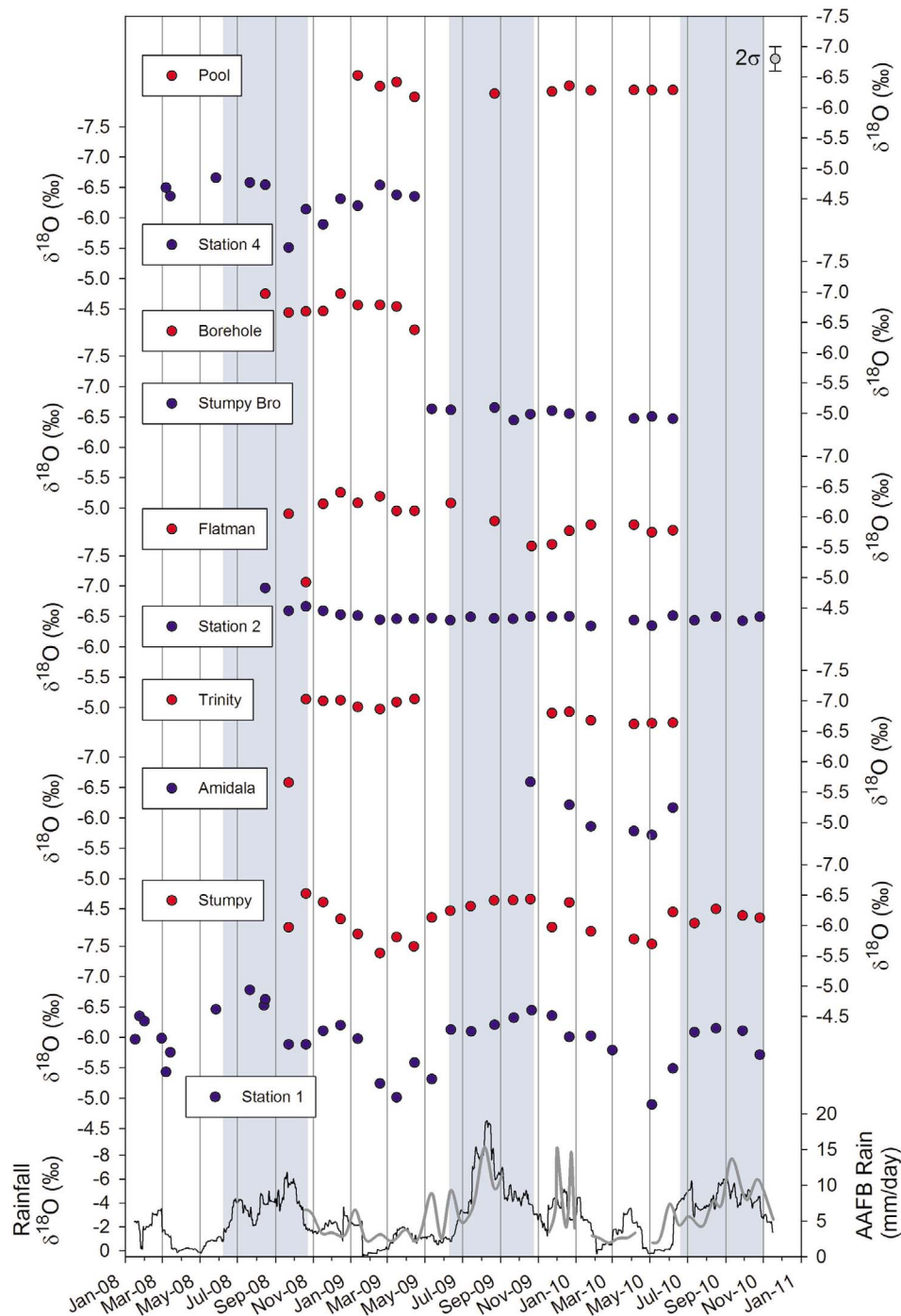
Figure 4. Comparison between cave dripwater $\delta^{18}O$ variations, smoothed rainfall $\delta^{18}O$ (dark gray line) and precipitation rate (black line) at Guam. Blue bars represent wet season. Three of the ten dripwater sites in Jinapsan Cave capture an annual cycle in dripwater $\delta^{18}O$ (Station 1, Stumpy and possibly Amidala), implying a dripwater residence time of <12 months. Limited annual variability in dripwater $\delta^{18}O$ at the seven other sites implies a dripwater residence time of >12 months Precipitation rate at Anderson Air Force Base (AAFB; 31 day running mean over 2008–2010).
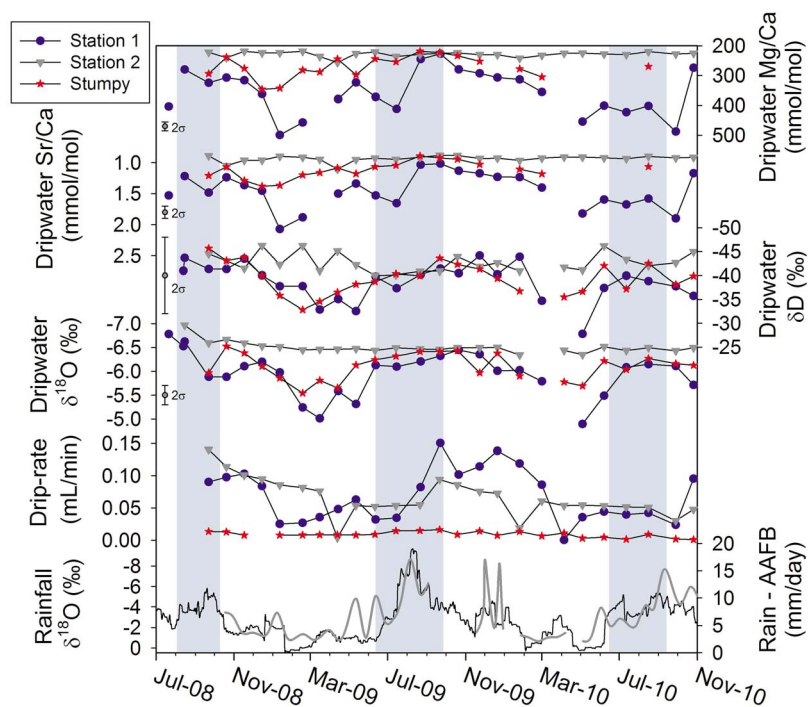
Figure 5. Geochemical variability in cave dripwater (Mg/Ca, Sr/Ca, δD, and $\delta^{18}O$) at three sites in Jinapsan Cave (Station 1, blue circle; Station 2, green triangle; Stumpy, red star). Note that $\delta^{18}O$, Sr/Ca, and Mg/Ca are plotted on inverted axes so that inferred wet conditions are upwards. Also plotted is smoothed rainfall $\delta^{18}O$ (dark gray line) and precipitation rate (black line) at AAFB (31 day running mean over 2008–2010). Vertical blue bars denote the wet season, as calculated when 5–6 pentads out of 8 fall above (onset) or below (retreat) the annual mean. Dripwater Mg/Ca and Sr/Ca display a seasonal cycle, most likely due to prior calcite precipitation (PCP) [*Fairchild et al.*, 2000]. The amount effect drives the seasonal cycle in dripwater $\delta^{18}O$ and δD. Drip-rate responds directly to rainfall via hydraulic loading. Two drips, Stumpy and Station 1, exhibit the strongest seasonal cycles.

et al., 1993; *Gat*, 1996]. The amount effect explains 57% of the variance in rainfall $\delta^{18}O$ (Figure 2). The slope of the regression yields a conversion of a decrease of 71 mm/month per 1‰ increase in rainfall $\delta^{18}O$ (±15 mm/month calculated using 95% bootstrap confidence interval) on monthly timescales, or 0.85 m/year per 1‰ rainfall $\delta^{18}O$ (Figure 2). Annual rainfall data for the 5 complete climatological GNIP years depict an inverse relationship, where the regression yields estimates of 1.1, 1.4, and 0.8 m/year per 1‰ rainfall $\delta^{18}O$ for mean, weighted mean, and wet season only, respectively (Figure 3b).

3.3. Cave Dripwater Data

3.3.1. Stable Isotopic Composition

[11] Cave dripwater stable isotopic composition loosely resembles rainfall composition variability in that some drips contain an annual cycle (Figure 4). At Station 1, wet season dripwater $\delta^{18}O$ is −6.5‰, whereas in the dry season dripwater $\delta^{18}O$ is −5.0‰ yielding an annual cycle of 1.5‰. At Stumpy, wet season $\delta^{18}O$ is −6.5‰, while dry season $\delta^{18}O$ is −5.5‰ yielding an annual cycle of 1.0‰. For the majority of the drips, dripwater $\delta^{18}O$ is around −6.2 to −6.5‰. The drips with minimal annual cyclicity have close to the same values and limited annual variation as the pool of water at the bottom of the cave (−6.4‰). The pool likely represents phreatic water composition, which results from the integration of water from the vadose zone.

[12] Interannual variability is observed in dripwater $\delta^{18}O$ at Station 1 and Stumpy (the site above the stalagmite referred to in this paper), in both the 2010 wet and dry seasons. The dry season of 2010 (~three months long) was drier than 2009 (~four months long), resulting in a smaller contribution of enriched $\delta^{18}O$ and δD to dripwaters at Station 1. Additionally, the wet season of 2010 is drier than 2009 at Station 1 resulting in more positive dripwater $\delta^{18}O$ and δD at Station 1 during the wet season of 2010 (−6.6‰) compared to 2009 (−6.1‰). Although this change is within analytical error, it is replicated over several months (Figure 5).
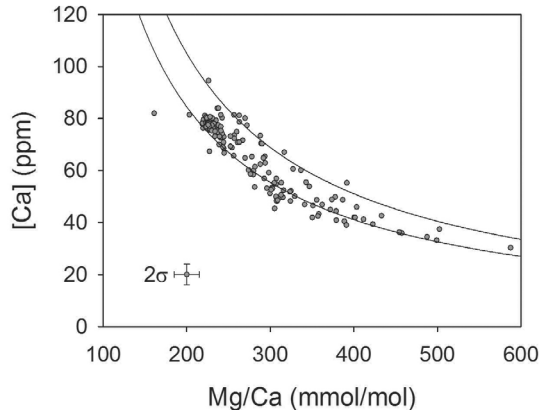
Figure 6. Calcium concentration in cave dripwater [Ca] versus Mg/Ca for all drips in Jinapsan Cave collected Aug 2008-Dec 2010. Curves represent modeled lines of prior calcite precipitation (PCP) that can alter dripwater geochemistry [*Fairchild et al.*, 2000]. Dry season values occupy the lower, right region of the plot – lower [Ca] and higher Mg/Ca. Dripwater geochemical behavior closely follows that predicted by the PCP hypothesis.

3.3.2. Trace Metal Ratios

[13] Just as stable isotopic values in rainfall and some cave dripwaters differ between wet and dry seasons, trace metal ratios (Mg/Ca and Sr/Ca) in cave dripwaters can also reflect changes in the annual hydrologic cycle. While most sites do not show a seasonal signal in dripwater composition, two sites (Station 1 and Stumpy) show clear variability at the sub-annual scale. At Station 1, trace metal ratios exhibit the largest annual variability and greatest values during the dry season (Mg/Ca dry season ≈ 450; Mg/Ca wet season ≈ 200 mmol/mol). Stumpy has the second largest wet/dry season cycle (Mg/Ca dry season ≈ 350; Mg/Ca wet season ≈ 200 mmol/mol). Two other sites resemble Stumpy (Figure 5) with muted seasonality (Trinity and Amidala), while the remaining drip sites resemble Station 2 (Figure 5), showing no annual cycle and low trace metal ratios (Mg/Ca ~200–240 mmol/mol year-round).

[14] Changes in trace metal ratios in Jinapsan cave dripwaters are consistent with the theory of prior calcite precipitation (PCP) [*Fairchild et al.*, 2000]. During the dry season, voids may open in the bedrock which would allow for CO_2 to degas, thus causing more calcite to precipitate along a flow path [*Fairchild et al.*, 2000]. Because the distribution coefficient for Mg in calcite is ≪1 (~0.04) [*Huang and Fairchild*, 2001], the water remaining after calcite precipitation becomes enriched in Mg

relative to Ca, thus trending toward higher Mg/Ca ratios. Conversely during the wet season, voids in the bedrock fill with water inhibiting CO_2 from degassing, and thus causing Mg/Ca ratios to decrease as less calcite precipitation occurs before water reaches the stalagmite surface. Guam dripwater trace metal ratios closely follow the trend predicted via PCP (Figure 6).

3.4. Cave Dripwater Geochemistry and Rainfall Relationship

[15] At Guam, annual and interannual changes in rainfall $\delta^{18}O$ correlate with rainfall amount (Figures 2 and 3). The regression-based estimate of 1‰ change in rainfall $\delta^{18}O$ for every 71 ± 15 mm/month change in rainfall confirms that the "amount effect" controls the annual cycle of precipitation at the site, and the smoothed time series demonstrates that this relationship holds at interannual timescales (Figures 3a and 3b). Preliminary results from the stalagmite suggest that the amount effect also operates over decades to centuries at this tropical site (see section 3.10 and Figure 9 for a more in-depth discussion). At decadal and longer timescales, it is also possible for source changes to alter rainfall isotopic composition [*Aggarwal et al.*, 2004]. Proper assessment of the potential role of source changes is beyond the scope of this study and requires: 1) an array of stalagmite $\delta^{18}O$ time series across the Pacific that cover a coeval time period and 2) GCMs that include rainfall isotopic composition.

[16] Cave dripwaters record changes in rainfall, although some sites provide a more robust record of seasonal or intra-annual rainfall variability than others. The geochemistry records from Station 1 display the largest annual cycle amplitude of all sites, followed by the records from the Stumpy site. No other drip sites capture the annual cycle in rainfall, with the possible exception of Amidala. This evidence suggests that, independent of the geochemical variable, the ability of a given drip site to record the annual cycle is most likely dependent upon the specific architecture of preferential pathways taken by groundwater as it moves through the overlying bedrock and emerges from individual locations in the cave ceiling. No relationship is observed between drip-rate and strength of annual cyclicity (Figure 5), ruling out a simple physical argument for dripwater geochemical response. The bedrock (Mariana Limestone) is triple-porosity karst rock, and vadose water travels in preferential pathways with various lengths and conductivities to individual drip sites in the cave [*Jocson et al.*, 2002]. There likely exists a continuum

of drips within the cave from those recording a strong annual cycle to no annual cycle, with the no annual cycle response dominating the sites chosen during this study. The $\delta^{18}O$ rainfall record was smoothed with a 7-month amount-weighted running mean (Figure 3) to approximate the effects of bedrock integration. The range of smoothed rainfall $\delta^{18}O$ variability is greater than the range of dripwaters suggesting a residence time between 7 and 12 months for Station 1 and Stumpy (and possibly Amidala) and greater than 12 months for all others.

3.5. Drip-Rate and Groundwater Residence Time

[17] Drip-rates in all drips respond to the hydrologic loading during the rainy season by increasing discharge at the drip, however not all drips vary seasonally. Using drip-rate criteria to define a seasonal drip, only sites Station 1, Stumpy, Station 4, and Amidala have relative standard deviations of discharge >50%, assigning them as seasonal drips [*Smart and Friederich*, 1986; *Baker et al.*, 1997; *Fairchild et al.*, 2006]. All other drips have a relative standard deviation of drip-rate <50%, assigning them as seepage flow [*Smart and Friederich*, 1986; *Baker et al.*, 1997; *Fairchild et al.*, 2006].

[18] Interestingly, three of the four drips that are categorized as seasonal based on drip-rate changes also display an annual cycle in dripwater geochemistry, whereas the other drips categorized as seepage do not contain an annual cycle in dripwater geochemistry. Stumpy and Station 1, contain a clear annual cycle in $\delta^{18}O$, δD and Mg/Ca (Figure 4). A third site, Amidala, might preserve an annual signal in $\delta^{18}O$ and δD, but additional data are needed. The fourth site, Station 4, categorized as seasonal did not display a geochemical annual cycle. As a result of the muted $\delta^{18}O$ variability during the wet season, two of the original drip sites were abandoned in April 2009 (Station 4 and Borehole) in order to identify additional sites that display a higher amplitude annual cycle in dripwater geochemistry (Figure 4). Collection at drip sites Stumpy's Brother and Amidala began in May 2009, leaving the number of observed drip-sites static (Figure 1).

[19] In the drips displaying an annual cycle in dripwater geochemistry, variability in cave dripwater $\delta^{18}O$ shows a muted response compared to rainfall variability as the reservoir in the overlying bedrock acts to dampen the short-term variations in the stable isotopic signal in rainfall. At the seepage flow sites, long residence times may completely mute the annual cycle (Figure 4). As a result, each drip

outputs a weighted average of rainfall composition that is dependent upon bedrock residence time.

[20] Estimates of residence time are calculated based on estimates of overlying bedrock volume, porosity, number of drips in the cave ceiling, drip-rate (or discharge), and recharge. While it is difficult to know the exact values, reasonable assumptions are made to provide a rough estimate of residence time. The detailed survey of the cave, small size, and simple bedrock geometry allow for a quantitative estimate of bedrock volume (Figure 1). The distance from cave entrance to the pool at the bottom is ~43 m. The overlying surface has an angle upward that is very similar to the cave (downward) making a cone of bedrock above the cave. The volume is estimated at ~39,900 m³. Estimates of porosity are taken at 30 and 45%, which serve as upper and lower bounds for karst composed of young coral limestone [*Vacher and Mylroie*, 2002]. Lower porosity would act to shorten residence time. Two values of average drip site density were used, 100 and 200 cm spacing between drips, to provide rough estimates of total discharge. Given the ceiling surface area (680 m²), the two estimates of 100 and 200 cm spacing equals a total number of 67,900 and 17,000 total drips in the cave, respectively. The drip-rate was measured at all sites and ranges from 0.001 to 5 mL/min with an average for all 9 sites of 0.7 mL/min (N = 103). Recharge is assumed to occur during the entire year, though this is probably not the case (see section 3.6 for further discussion). Using various combinations of the above estimates yield residence times from 5 months to 34 years. Using the combination of 45% porosity (high estimate), 0.7 mL/min (average drip-rate), and 200 cm spacing, or 17,000 drips (low total number), yields a residence time of 35 months. Given the conical geometry of the overlying bedrock, variable drip rates recorded and variable porosity of karst limestone [*Bakalowicz*, 2005], residence times are site specific and highly heterogeneous but likely lie somewhere between many months to several years in Jinapsan cave.

[21] Cave dripwater $\delta^{18}O$ acts as a natural tracer to provide supporting evidence for groundwater residence time. Given the annual cycle observed in dripwater $\delta^{18}O$ and δD, the residence time at sites Station 1 and Stumpy is likely subannual. A residence time substantially greater than 12 months would require minimal mixing in the bedrock for these drips to completely average out the annual cycle in rainfall composition. Also, it would take a fortuitous residence time that is a multiple of 12 such that the discharge for the drips occurs

during the proper season. Given that Guam receives 2–3 m of rain each year, and the shallow thickness of the overlying bedrock (42 m at the back to ~2 m at the front), there is no place to store such an amount of water in the bedrock. The higher average drip-rate, or discharge, at Station 1, 0.07 mL/min, compared to Stumpy, 0.009 mL/min, suggests that Station 1 has a higher volume of water in the bedrock that Stumpy as they have similar residence times. Sites like Trinity (average drip-rate of 2.8 mL/min), Borehole (2.4 mL/min), and Flatman (0.2 mL/min) must have much larger volumes of water in the karst as they have higher discharge and little geochemical variability on the annual timescales, indicating residence times between 1 to ~10 years.

3.6. Effective Recharge

[22] Cave dripwater $\delta^{18}O$ is consistently more negative than mean annual rainwater $\delta^{18}O$ indicating recharge is more effective in the wet season than in the dry season. Weighted mean annual $\delta^{18}O$ at Station 1 is −6.1‰ for the period from December 2008 to November 2009 and −5.9‰ from December 2009 to November 2010. Rainwater compositions over the same periods are −5.2‰ and −4.2‰ respectively, indicating that effective recharge occurs more during the wet season, when isotopic values are typically more negative than during the dry season. One potential cause for this effect is the increased demand for moisture by plants during dry months when precipitation is less available. In a karst landscape, conduits can efficiently transport large volumes of water in a very short period of time, so the potential for precipitation to exceed infiltration and lead to overland flow may be diminished. The implication of this observation for the Northern Guam Lens Aquifer is that rains during the dry season do not seem to contribute to recharge, so the length or intensity of the wet season would be more critical for maintaining the water table. This observation agrees with a previous study that estimates that recharge mainly occurs during the months July to November [*Jones and Banner*, 2003]. Limited recharge during the dry season may also help to explain the limited annual cycle in dripwater $\delta^{18}O$ at sites Station 2, Flatman, Borehole, and Trinity. Recharge thresholds of approximately 150 to 200 mm/month are estimated based on the amount weighted rainfall $\delta^{18}O$ data and mean dripwater $\delta^{18}O$ data, in agreement with prior estimates [*Jones and Banner*, 2003].

[23] The deviation between stalagmite $\delta^{18}O$ and rainfall amount over the first decade of the 2000s

may be explained by the close passage of four tropical cyclones in ~2 years, including Super Typhoon Chataan (Figure 9). The effective recharge from extreme events may have been low in this cave system, which explains the lack of signature in the stalagmite $\delta^{18}O$, as values tend to be more positive from 1995 to 2005. Alternatively, the lack of preservation of a tropical cyclone signal may be due to activation of conduits in response to the large influx of water. Conduit waters have much shorter transit times, and have less chance to equilibrate with respect to calcite. Therefore, the precipitation from the cyclones may have reached the cave undersaturated and would therefore not be preserved in the speleothem. This deviation between rainfall and stalagmite $\delta^{18}O$ suggests that while the sites in Jinapsan Cave are well-equipped to resolve longer-term changes in rainfall, they are not well-suited to resolving extreme tropical cyclone events, in contrast to results for other tropical speleothems [*Frappier et al.*, 2007]. This conclusion for the cave is supported by preliminary data from Dec. 2009 where the rainfall $\delta^{18}O$ composition of a tropical cyclone is measured to be −8.6‰, but a corresponding perturbation in dripwater $\delta^{18}O$ is not observed at any of the sites in Jinapsan Cave.

3.7. Stalagmite Age Model

[24] We investigated the possibility of using cyclicity in Mg/Ca ratios as chronological constraints to construct an age model by postulating that they represent annual cycles (Figure 7). The U-Th date measured on Stumpy provides average age control on the portion overlapping in the instrumental era; 1866 year CE ± 18 years at a depth of 6.3 mm. This date and depth yields an average growth rate of 45 μm/year. Visual counting of the cycles in Mg/Ca provided an estimate of 110–144 cycles (inferred years) at the same depth as the U-Th date, depending upon how conservative the subjective cycle identification was (Figure 7). The Mg/Ca estimation (110–144 years) is consistent with the U-Th date (140 years before 2005, or 1866 year CE, ±18 years), however the error of the date is not reduced. The linear, continuous presence of Mg/Ca cycles suggests uniform growth over the last 160 years without any signs of a hiatus or nonlinearity in growth (Figure 7). Despite attempts to filter the time series and estimate growth conditions, a MATLAB peak counting program [*Smith et al.*, 2009] and wavelet analysis did not improve cycle counting accuracy, most likely due to low frequency components to the time series and low signal-to-noise of the annual cycle. The Mg/Ca cycle signal is likely complicated
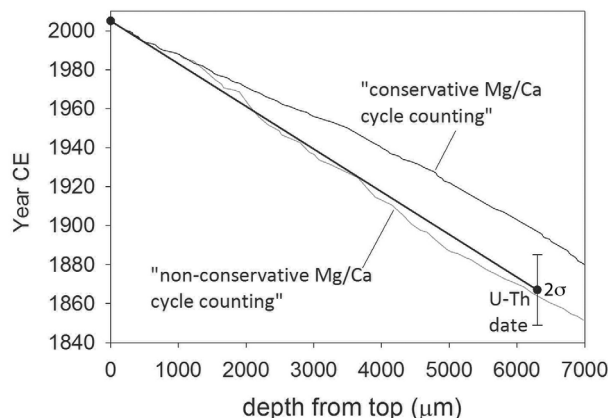
Figure 7. Three age models for stalagmite "Stumpy" based on a U-Th age (black line) and Mg/Ca cycle counting (gray curve and black curve). The Mg/Ca age model is based on the less conservative count of 144 years (gray curve), versus 110 years (black curve), to more closely match the U-Th age. Therefore, two age models predict a similar age for the 6300 μm horizon of ~140 years ago. The Mg/Ca cycle counting models both suggest a fairly linear and continuous growth of the stalagmite over the last 160 years.

by interactions between rainfall, water-rock interaction, and hydrologic flow path changes, making it difficult to employ Mg/Ca cycles as an absolute chronometer. Additionally, the growth rate of the stalagmite at 45 μm/year is relatively slow and does not represent an ideal candidate for producing a calibration over the instrumental era, but so far it is the best candidate found in Jinapsan Cave.

[25] The poor ability of Mg/Ca to construct an age model (Figures 7 and 9 and Figure S1 in Text S1) could be due to periods of increased rainfall during the dry season resulting in 'missed' years. Increased dry season rainfall prevents voids in the bedrock from drying up and allowing CO_2 to degas PCP to occur. This reduces or eliminates the seasonality in Mg/Ca, as the dry season would not have higher Mg/Ca. Random skipped seasons are also documented in other annual stalagmite records [*Roberts et al.*, 1998; *Treble et al.*, 2003, 2005b; *Desmarchelier et al.*, 2006; *Johnson et al.*, 2006; *Smith et al.*, 2009]. Additionally, non-uniform growth bands thickness across the width of the stalagmite, as demonstrated in the $\delta^{18}O$ transects (Figure 8) and multiple laser ablation scans (Figure S1 in Text S1), suggest sub-mm-scale variability in calcite growth layers that could cause annual bands to pinch out leading to "missed" years.

[26] Additional temporal uncertainty in the $\delta^{18}O$ and Mg/Ca profiles may be due to the fact that the $\delta^{18}O$ paths and laser ablation scans were analyzed

on mirror halves of the sample. Variations in growth layers may lead to apparent differences in the $\delta^{18}O$ versus the Mg/Ca time series. Ideally it would be best to mill for $\delta^{18}O$ on the same half as the laser ablation scans. However, this milling is difficult as the sample is cut to a small dimension to fit into the laser ablation cell, and the width of the $\delta^{18}O$ track is much wider than the laser spot size.

3.8. Non-traditional Hendy Tests

[27] A moderate correlation between $\delta^{18}O$ and $\delta^{13}C$ in the stalagmite time series suggests that non-equilibrium effects could influence calcite isotopic composition; however other evidence suggests equilibrium effects dominate the signal. The correlation between $\delta^{18}O$ and $\delta^{13}C$ is moderate in stalagmite sample Stumpy ($R^2 = 0.42$), suggesting that non-equilibrium effects could influence $\delta^{18}O$ [*Hendy*, 1971; *Mickler et al.*, 2006]. However, parallel tracks drilled 6 mm apart in Stumpy, one down the center and one closer to the edge have the same mean and variability in $\delta^{18}O$ despite the fact that the track in the middle covered half as much distance per unit time as the side track (Figure 8). The parallel tracks demonstrate that non-equilibrium effects are likely minimal in this sample. Also, the middle track, located in the traditional growth axis, appears to not contain the most recent part of the record and misses
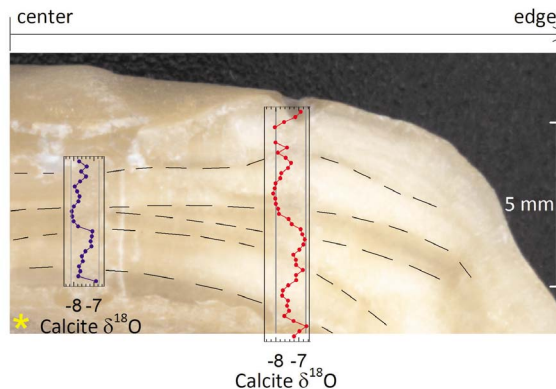

Figure 8. Parallel tracks drilled for stalagmite $\delta^{18}O$ measurements on the top-most portion of stalagmite "Stumpy." Isochron $\delta^{18}O$ measurements, dashed lines connecting $\delta^{18}O$ transects, have the same $\delta^{18}O$ values indicating that the sample passes the Hendy test and kinetic fractionation of stalagmite calcite is likely minimal in this sample. However, complicated banding in this region presents a difficult scenario to drill a traditional Hendy test, and the authors endorse drilling parallel paths instead of discrete points in this situation to test for equilibrium precipitation of stalagmite calcite.
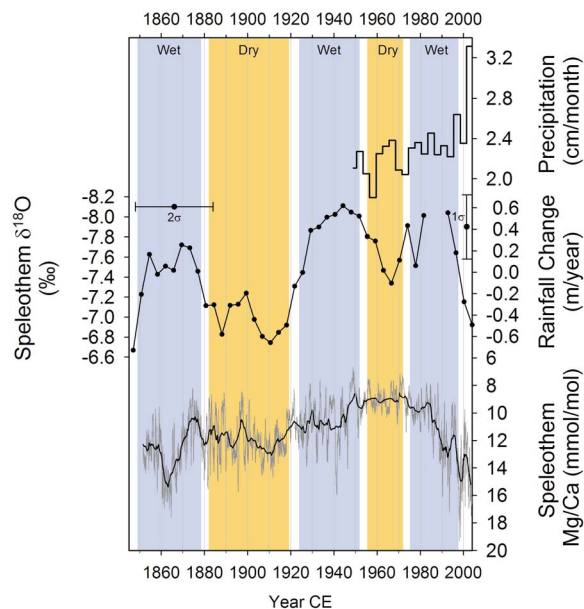
Figure 9. Summary plot of rainfall rate (NOAA GHCN data), speleothem Mg/Ca of "Stumpy" (graph inverted) below dripsite Stumpy ("ST," Figure 1) measured via Laser Ablation-ICPMS, and speleothem $\delta^{18}O$ of Stumpy (also inverted). Rainfall change is converted from stalagmite $\delta^{18}O$ using the mean value of six different methods (section 3.9). Error bars are the analytical error of the U-Th date and the ± 0.3 m/year error for the stalagmite to rainfall $\delta^{18}O$ conversion (computed in section 3.9). Higher stalagmite $\delta^{18}O$ and Mg/Ca indicate drier conditions (orange bars), and lower stalagmite $\delta^{18}O$ and Mg/Ca indicate wetter conditions (blue bars). Inferred dry periods occur from 1880 to 1930, 1950–1975, and 1995–2005. The 1880–1930 drought is the most pronounced dry period over the last $\sim$160 years, and it lasts for $\sim$50 years.

some information in the middle of the track. The growth bands in the sample bend and pinch visually, which is reflected in the $\delta^{18}O$ record. Furthermore, if a traditional "Hendy Test" were drilled on the sample, it may have been identified as a false positive for failing the test, as it is extremely difficult to sample the same period of time on the edges where bands pinch [*Mickler et al.*, 2006; *Dorale and Liu*, 2009]. Analyzing parallel paths is a more thorough method for testing non-equilibrium effects on a stalagmite than drilling spots along a growth layer, albeit slightly more time consuming. Scientists who wish to study stalagmites containing non-uniform growth banding (i.e., unconformities where one cannot easily trace the growth layers as in Figure 8), may choose to sample the best portion of calcite that covers the most time – even if it is not located in the center of the stalagmite, as long as parallel tracks reproduce the $\delta^{18}O$ signal. This greatly increases the percentage of samples collected in the field that can

be used for paleoclimate studies, as many samples have complex growth patterns. It is of note that coarser resolution transect of these two regions, i.e., transects drilled at lower spatial resolution, would reproduce the mean and variability in stalagmite $\delta^{18}O$ and yield internally consistent paleoclimate reconstructions. These results suggest care should be taken when choosing both where to drill a stalagmite for a paleoclimate time series, as well as the spatial resolution at which to drill the sample.

3.9. Rainfall Amount: Rainfall $\delta^{18}O$ Transfer Function

[28] We use six methods to calculate a transfer function between rainfall amount and rainfall $\delta^{18}O$. Method 1: using all of the GNIP monthly rainfall $\delta^{18}O$ data, we calculate a conversion of 71 ± 15 mm/month, or 0.85 ± 0.18 m/year, per 1‰ $\delta^{18}O$ (error calculated via bootstrap confidence intervals). Methods 2 and 3: as this study suggests that recharge primarily occurs during the wet season months (see section 3.6), thresholds of >150 mm/month and >200 mm/month of rainfall yield a regression of 0.71 and 0.79 m/year of rainfall per 1‰ $\delta^{18}O$, respectively. Method 4: annual mean rainfall $\delta^{18}O$ for the five complete climatological years (April to March) of GNIP data yields a conversion of 1.1 m/year per 1‰ $\delta^{18}O$. Method 5: using the amount weighted rainfall $\delta^{18}O$ for the five complete climatological years of GNIP data yield a regression of 1.4 m/year per 1‰ $\delta^{18}O$. Method 6: using wet season only (May – October) for the 5 climatological years of GNIP data yields a regression of 0.8 m/year per 1‰ $\delta^{18}O$. Given the range of values calculated via six different methods, we estimate that the conversion from rainfall amount to rainfall $\delta^{18}O$ is an increase (decrease) of $\sim$0.95 $\pm$ 0.3 m/year per 1‰ decrease (increase) in $\delta^{18}O$ (mean and standard deviation of the six methods).

3.10. Paleo-Rainfall and Variations in Stalagmite Geochemistry

[29] Geochemical records of stalagmite Mg/Ca and $\delta^{18}O$ (Table S1 in Text S1) were generated to cover the last $\sim$160 years from stalagmite 'Stumpy' (Figure 9). The sub-annual record of stalagmite Mg/Ca ratios shows periods where cycles are clearly evident (1850–1910; 1920–1950; 1980–2000, based on the U-series age) and periods where cycles are ambiguous (1910–1920; 1950–1980). We speculate that these cycles are annual in origin, but dating uncertainty precludes a more definitive statement about the periodicity of these cycles. Decadal variability in

stalagmite Mg/Ca occurs throughout the record and is sometimes coeval with amplitude reduction in the higher frequency cycles. The resolution of the stalagmite $\delta^{18}O$ record (~4 years/sample) from Stumpy is insufficient to resolve annual cycles, which results in decadal changes dominating the record. Higher stalagmite $\delta^{18}O$ values occur from 1875 to 1925, 1955–1975, and 1995–2005, when the Mg/Ca cycles are less clear.

[30] Stable isotopic variations in rainfall (Figure 3) and dripwater (Figure 4) suggest that interplay between dry season duration/intensity and wet season duration/intensity drive the annual cycle amplitude, and consequently interannual variability in the high-resolution data. For example, the dry seasons of 1963 and 1964 are above average in rainfall and display the most negative rainfall $\delta^{18}O$ values in the rainfall record, resulting in minimal seasonality and interannual variability when compared with the rest of the GNIP data from the 1960s and 70s (Figure 3). In a corresponding example from the cave dripwater data, the relatively shorter dry season of 2010 has a briefer period of more positive $\delta^{18}O$ and δD values, as compared to 2009 (Figure 5). In a multiyear resolved time series, shorter dry seasons would lead to more negative $\delta^{18}O$ values in both cave dripwater and stalagmites in terms of both the amount effect and from less effective recharge of the more positive rainfall $\delta^{18}O$ that falls during the dry season. Wet season $\delta^{18}O$ values appear to saturate at ~−8‰, so any month with precipitation in excess of ~525 mm (calculated using regression equation) would not substantially change $\delta^{18}O$. However, the length of the wet season could impact dripwater geochemistry as higher effective recharge of wet season rains would lead to a more depleted $\delta^{18}O$ signature of the wet season in the integrated water in the bedrock. Generally, a longer wet season complements a shorter dry season, and cave dripwater and stalagmites would have more negative $\delta^{18}O$ via both the amount effect and higher effective recharge under these conditions. Last, comparison of stalagmite $\delta^{18}O$ with rainfall station data from Anderson Air Force Base, Guam (Figure 9) agrees with previous estimates of the transfer function between amount and rainfall $\delta^{18}O$. Binning annual average rainfall into three-year bins in order to approximate the resolution of the stalagmite reveals that the peak to trough difference in stalagmite $\delta^{18}O$ for the 1980s minus 1960s of ~0.6‰ corresponds to ~0.6 m/year of rainfall change. The agreement between this estimate and those in section 3.9 suggests that the amount effect operates on decadal timescales in Guam under the relatively static boundary conditions for the last 160 years (sea level, ice volume,

temperature, etc.). Although on millennial to orbital timescales, this relationship may not be stationary, and isotope-enabled GCM output could be a reliable method to resolve stationarity of stable isotopes in proxy data.

[31] We postulate three general scenarios to explain how changes in rainfall cause geochemical variables to deviate from the computed climatology over the course of a year: 1) uniform change of the annual mean, no change in seasonality with both wet and dry seasons equally affected, 2) increase or decrease of dry season duration including intermittent rains, wet season unchanged, and 3) increase or decrease of wet season duration including intensity changes, dry season unchanged. Scenario 1 is unlikely because rainfall records over the last 60 years suggest that this scenario did not take place. Instead, Scenarios 2 and 3 represent more likely ways by which rainfall variability occurs. In a rainfall time series, Scenario 2 causes dry season troughs to pinch out, or become shallower, leading to a reduction in seasonality. These years would reduce the amplitude of any annual cycle in cave dripwaters and stalagmite trace metal ratios, as observed in 2010, and have more negative stable isotopic compositions. Under Scenario 3, wet season peaks in a rainfall time series would have a broader shape during a longer wet season. This change in the seasonal cycle would not affect the annual cycles in the trace metal ratios of the stalagmite, as values tend to saturate at a wet season value when no PCP occurs (Figure 5). However, cave dripwaters would have more effective recharge of the negative isotopic rainfall, and hence, more negative stable isotopic composition in the bedrock integrated waters. Also, were the wet season to be less intense, the trace metal ratios would likely not reflect the rainfall reduction, as generous rainfall occurs regardless, but the stable isotopic composition would increase. Therefore, trace metal ratios are more sensitive to dry season changes, whereas $\delta^{18}O$ and δD are sensitive to changes in both wet and dry seasons.

[32] Changes in the amplitude of the annual cycle of the trace metal ratios in stalagmite calcite likely reflect changes in rainfall seasonality, whereas decadal-scale changes reflect a combination of rainfall and hydrology changes. Theoretical calculations of calcite compositions based on the Mg/Ca measured in the Stumpy dripwater and a distribution coefficient (D_{Mg}) of 0.04 [*Huang and Fairchild,* 2001] yield values that match the absolute value and range of variability in the stalagmite Mg/Ca. Therefore, we interpret calcite Mg/Ca variability to indicate changes in dripwater Mg/Ca driven by PCP. Due to uncertainty in the actual forcing causing

proxy variability and uncertainty in growth rate, however, a quantification of the relationship between rainfall amount and stalagmite Mg/Ca is not possible. Nonetheless, periods of reduced amplitude (1910–1920; 1950–1980) may indicate reduced seasonality either through above-average dry seasons or below-average wet seasons. Decadal-scale decreases in Mg/Ca (1875–1900; 1900–1925; 1980–2005) reflect both a decrease in rainfall and hydrologic changes in the epikarst.

[33] Hydrologic changes associated with changes in flow path of water through the overlying bedrock may also affect dripwater and stalagmite trace metal ratios, which is not strictly interpreted as a change in rainfall amount. For example, a change in water flow path through the bedrock may mix waters between Stumpy and Station 2 – a plausible scenario given that the two sites are only two meters apart. As Station 2 has lower Mg/Ca ratios than Stumpy and no annual cyclicity, this mixing would lead to decadal and possibly longer changes in dripwater and stalagmite trace metal ratios in Stumpy (lower average values) and a possible reduction in annual cyclicity, such as during the time period 1950–1980. While rainfall changes force the changes in flow path of water through the bedrock, the geochemical reactions resulting from the change in flow path through bedrock would dominate the decadal-scale geochemical response.

3.11. Stalagmite Reconstruction of Past Rainfall

[34] Decadal changes in stalagmite $\delta^{18}O$ and Mg/Ca over the last ~160 years suggest pronounced alternations between wet and dry periods (Figure 9; blue and orange regions, respectively). Uncertainties in the age model do not allow for quantification of the periodicity of the decadal cycles, an inferred linear and continuous age model qualifies the cycles as decadal in origin. Three dry climatic periods (1875–1900; 1900–1925; 1955–1975) provide three different situations to illustrate how the combination of $\delta^{18}O$ and Mg/Ca yield additional insights on rainfall variability at Guam (Figure 9). The following relationships facilitate the interpretation of the stalagmite record: high $\delta^{18}O$ = reduction in rainfall, high Mg/Ca = dry dry-seasons, high Mg/Ca seasonality suggests a large difference between wet and dry season (i.e., relatively wet wet-seasons and dry dry-seasons). We interpret high $\delta^{18}O$, high Mg/Ca variability, and high Mg/Ca values from 1875 to 1900 (Figure 9) to indicate a dry climate caused by long dry seasons. From 1900 to 1925 (Figure 9),

high $\delta^{18}O$, low Mg/Ca variability, and high Mg/Ca values equate to drying caused by markedly decreasing wet season rainfall. However, seasonality also decreases as a consequence of the dry season appearing wetter in contrast to the "dry" wet season. From 1955 to 1975 (Figure 9), high $\delta^{18}O$, low Mg/Ca variability, and low Mg/Ca values equate to moderate drying during the wet season, with somewhat wetter dry season – with yearly rainfall having an overall decrease. Although tempting, dating error (±18 years) precludes the matching of high stalagmite $\delta^{18}O$ values in the 1960s to the low rainfall recorded in the 1950s. Additionally, the 1960s have muted seasonality in Mg/Ca, and $\delta^{18}O$ increases, which may be due to the mixing of Station 2 (lower Mg/Ca) and Station 1 (higher Mg/Ca) waters during this period of above average rainfall. Outside of dating errors, the dry period from 1875 to 1925 (Figure 9) was extended in duration and most likely driven by long, intense dry seasons – a scenario that does not resemble rainfall experienced over the last 80 years of the record. Indeed, the wet period from 1930 to 1950 stands out as a remarkably above average rainfall and should not be viewed as normal conditions for Guam. The dry period from 1875 to 1925 represents a much stronger drought than the 1950s drought. Water resource managers on Guam should incorporate decades of relatively less rainfall into their planning, especially given that the island has a rapidly increasing population that is dependent on the fresh water aquifer.

4. Conclusions

[35] The relationship between rainfall (amount, $\delta^{18}O$) and cave dripwater ($\delta^{18}O$, Mg/Ca, Sr/Ca) provide a transfer function to reconstruct past hydrologic changes on the island of Guam, located on the northeast perimeter of the Western Pacific Warm Pool. The "amount effect" relationship explains ~57% of the variance in the $\delta^{18}O$ of Guam rainfall. The inverse relationship between rainfall amount and $\delta^{18}O$ composition in Guam yields a conversion of a decrease (increase) of 0.94 ± 0.3 m/year for every 1‰ increase (decrease) in rainfall $\delta^{18}O$. Annual cycles in cave dripwater $\delta^{18}O$, δD, Mg/Ca and Sr/Ca were present only at sites Station 1 and Stumpy (and possibly Amidala), whereas the other sites monitored have limited annual variability. The amplitude of annual cycles in cave dripwater $\delta^{18}O$ was larger in 2009 compared to 2010 due to greater seasonal contrast in precipitation amount in 2009 versus 2010. Trace metal ratios in

cave dripwaters follow the prediction based on prior calcite precipitation (PCP), and dry season variability appears to control trace metal ratio composition. The age model for the stalagmite sample based on both U-Th dating and Mg/Ca cycle counting suggest linear and continuous growth over the last 160 years for the upper 7 mm, yielding an average growth rate of 45 μm/year. Alternating decades of inferred wet and dry periods dominate the stalagmite δ^{18}O record, however age model errors do not allow for a quantification of the periodicity. According to the Guam stalagmite record, decades of relative drought occurred in ~1875–1925, 1955–1975, and 1995–2005, in which 1875–1925 drought was especially dry (0.65 ± 0.3 m/year below average) and prolonged, and may serve as a worst-case scenario for water planners in Guam, at least until a longer record is available. This stalagmite record highlights the natural hydrologic changes that a tropical, rainy site in the WPWP may experience, which may be related to basin-scale hydrologic changes – however more records are needed to determine the extent of basin-wide decadal-scale changes.

Acknowledgments

References

Aggarwal, P. K., K. Frohlich, K. M. Kulkarni, and L. L. Gourcy (2004), Stable isotope evidence for moisture sources in the Asian summer monsoon under present and past climate regimes, *Geophys. Res. Lett.*, *31*, L08203, doi:10.1029/2004GL019911.

Bakalowicz, M. (2005), Karst groundwater: A challenge for new resources, *Hydrogeol. J.*, *13*(1), 148–160, doi:10.1007/s10040-004-0402-9.

Baker, A., W. L. Barnes, and P. L. Smart (1997), Variations in the discharge and organic matter content of stalagmite drip waters in Lower Cave, Bristol, *Hydrol. Processes*, *11*(11), 1541–1555, doi:10.1002/(SICI)1099-1085(199709)11:11<1541::AID-HYP484>3.0.CO;2-Z.

Baker, A., C. L. Smith, C. Jex, I. J. Fairchild, D. Genty, and L. Fuller (2008), Annually laminated speleothems: A review, *Int. J. Speleol.*, *37*(3), 193–206.

Banner, J. L., M. L. Musgrove, Y. Asmerom, R. L. Edwards, and J. A. Hoff (1996), High-resolution temporal record of Holocene ground-water chemistry: Tracing links between climate and hydrology, *Geology*, *24*(11), 1049–1053, doi:10.1130/0091-7613(1996)024<1049:HRTROH>2.3.CO;2.

Banner, J. L., A. Guilfoyle, E. W. James, L. A. Stern, and M. Musgrove (2007), Seasonal variations in modern speleothem calcite growth in central Texas, USA, *J. Sediment. Res.*, *77*(8), 615–622, doi:10.2110/jsr.2007.065.

Boch, R., C. Spotl, and S. Frisia (2011), Origin and palaeoenvironmental significance of lamination in stalagmites from Katerloch Cave, Austria, *Sedimentology*, *58*(2), 508–531, doi:10.1111/j.1365-3091.2010.01173.x.

Bradley, C., A. Baker, C. N. Jex, and M. J. Leng (2010), Hydrological uncertainties in the modelling of cave dripwater δ^{18}O and the implications for stalagmite palaeoclimate reconstructions, *Quat. Sci. Rev.*, *29*(17–18), 2201–2214, doi:10.1016/j.quascirev.2010.05.017.

Buhmann, D., and W. Dreybrodt (1985), The kinetics of calcite dissolution and precipitation in geologically relevant situations of karst areas: 1. Open system, *Chem. Geol.*, *48*(1–4), 189–211, doi:10.1016/0009-2541(85)90046-4.

Burns, S. J., D. Fleitmann, A. Matter, J. Kramers, and A. A. Al-Subbary (2003), Indian Ocean climate and an absolute chronology over Dansgaard/Oeschger events 9 to 13, *Science*, *301*(5638), 1365–1367, doi:10.1126/science.1086227.

Cane, M. A., A. C. Clement, A. Kaplan, Y. Kushnir, D. Pozdnyakov, R. Seager, S. E. Zebiak, and R. Murtugudde (1997), Twentieth-century sea surface temperature trends, *Science*, *275*(5302), 957–960, doi:10.1126/science.275.5302.957.

Clement, A. C., R. Seager, and M. A. Cane (2000), Suppression of El Niño during the mid-Holocene by changes in the Earth's orbit, *Paleoceanography*, *15*(6), 731–737, doi:10.1029/1999PA000466.

Cobb, K. M., J. F. Adkins, J. W. Partin, and B. Clark (2007), Regional-scale climate influences on temporal variations of rainwater and cave dripwater oxygen isotopes in northern Borneo, *Earth Planet. Sci. Lett.*, *263*(3–4), 207–220, doi:10.1016/j.epsl.2007.08.024.

Cravatte, S., T. Delcroix, D. X. Zhang, M. McPhaden, and J. Leloup (2009), Observed freshening and warming of the western Pacific Warm Pool, *Clim. Dyn.*, *33*(4), 565–589, doi:10.1007/s00382-009-0526-7.

Cruz, F. W., I. Karmann, O. Viana, S. J. Burns, J. A. Ferrari, M. Vuille, A. N. Sial, and M. Z. Moreira (2005), Stable isotope study of cave percolation waters in subtropical Brazil: Implications for paleoclimate inferences from speleothems, *Chem. Geol.*, *220*(3–4), 245–262, doi:10.1016/j.chemgeo.2005.04.001.

Dansgaard, W. (1964), Stable isotopes in precipitation, *Tellus*, *16*(4), 436–468, doi:10.1111/j.2153-3490.1964.tb00181.x.

Desmarchelier, J. M., J. C. Hellstrom, and M. T. McCulloch (2006), Rapid trace element analysis of speleothems by ELA-ICP-MS, *Chem. Geol.*, *231*(1–2), 102–117, doi:10.1016/j.chemgeo.2006.01.002.

Dorale, J. A., and Z. H. Liu (2009), Limitations of Hendy Test criteria in judging the paleoclimatic suitability of speleothems and the need for replication, *J. Cave Karst Stud.*, *71*(1), 73–80.

Epstein, S., R. Buchsbaum, H. A. Lowenstam, and H. C. Urey (1953), Revised carbonate-water isotopic temperature scale, *Geol. Soc. Am. Bull.*, *64*(11), 1315–1325, doi:10.1130/0016-7606(1953)64[1315:RCITS]2.0.CO;2.

Fairchild, I. J., and P. C. Treble (2009), Trace elements in speleothems as recorders of environmental change, *Quat. Sci. Rev.*, *28*(5–6), 449–468, doi:10.1016/j.quascirev.2008.11.007.

Fairchild, I. J., A. Borsato, A. F. Tooth, S. Frisia, C. J. Hawkesworth, Y. M. Huang, F. McDermott, and B. Spiro (2000), Controls on trace element (Sr-Mg) compositions of carbonate cave waters: Implications for speleothem climatic records, *Chem. Geol.*, *166*(3–4), 255–269, doi:10.1016/S0009-2541(99)00216-8.

Fairchild, I. J., C. L. Smith, A. Baker, L. Fuller, C. Spotl, D. Mattey, and F. McDermott (2006), Modification and preservation of environmental signals in speleothems, *Earth Sci. Rev.*, *75*(1–4), 105–153, doi:10.1016/j.earscirev.2005.08.003.

Fleitmann, D., S. J. Burns, U. Neff, M. Mudelsee, A. Mangini, and A. Matter (2004), Palaeoclimatic interpretation of high-resolution oxygen isotope profiles derived from annually laminated speleothems from Southern Oman, *Quat. Sci. Rev.*, *23*(7–8), 935–945, doi:10.1016/j.quascirev.2003.06.019.

Frappier, A. B., D. Sahagian, S. J. Carpenter, L. A. Gonzalez, and B. R. Frappier (2007), Stalagmite stable isotope record of recent tropical cyclone events, *Geology*, *35*(2), 111–114, doi:10.1130/G23145A.1.

Frisia, S., I. J. Fairchild, J. Fohlmeister, R. Miorandi, C. Spotl, and A. Borsato (2011), Carbon mass-balance modelling and carbon isotope exchange processes in dynamic caves, *Geochim. Cosmochim. Acta*, *75*(2), 380–400, doi:10.1016/j.gca.2010.10.021.

Fuller, L., A. Baker, I. J. Fairchild, C. Spotl, A. Marca-Bell, P. Rowe, and P. F. Dennis (2008), Isotope hydrology of drip-waters in a Scottish cave and implications for stalagmite palaeoclimate research, *Hydrol. Earth Syst. Sci.*, *12*(4), 1065–1074, doi:10.5194/hess-12-1065-2008.

Gat, J. R. (1996), Oxygen and hydrogen isotopes in the hydrologic cycle, *Annu. Rev. Earth Planet. Sci.*, *24*, 225–262.

Genty, D., A. Baker, and B. Vokal (2001), Intra- and inter-annual growth rate of modern stalagmites, *Chem. Geol.*, *176*(1–4), 191–212, doi:10.1016/S0009-2541(00)00399-5.

Griffiths, M. L., et al. (2009), Increasing Australian-Indonesian monsoon rainfall linked to early Holocene sea-level rise, *Nat. Geosci.*, *2*(9), 636–639, doi:10.1038/ngeo605.

Guilderson, T. P., and D. P. Schrag (1999), Reliability of coral isotope records from the western Pacific warm pool: A comparison using age-optimized records, *Paleoceanography*, *14*(4), 457–464, doi:10.1029/1999PA900024.

Hendy, C. H. (1971), Isotopic geochemistry of speleothems. 1. Calculation of effects of different modes of formation on isotopic composition of speleothems and their applicability as palaeoclimatic indicators, *Geochim. Cosmochim. Acta*, *35*(8), 801–824, doi:10.1016/0016-7037(71)90127-X.

Huang, Y. M., and I. J. Fairchild (2001), Partitioning of Sr^{2+} and Mg^{2+} into calcite under karst-analogue experimental conditions, *Geochim. Cosmochim. Acta*, *65*(1), 47–62, doi:10.1016/S0016-7037(00)00513-5.

Intergovernmental Panel on Climate Change (2007), *Climate Change 2007: The Physical Science Basis—Contribution of Working Group I to the Fourth Assessment Report of the Intergovernmental Panel on Climate Change*, edited by S. Solomon et al., 996 pp., Cambridge Univ. Press, Cambridge, U. K.

Jenson, J. W., T. M. Keel, J. R. Mylroie, J. E. Mylroie, K. W. Stafford, D. Taborosi, and C. Wexel (2006), Karst of the Mariana Islands: The interaction of tectonics, glacio-eustasy, and freshwater/seawater mixing in island carbonates, in *Perspectives on Karst Geomorphology, Hydrology, and Geochemistry—A Tribute Volume to Derek C. Ford and William B. White*, edited by R. S. Harmon and C. M. Wicks, *Spec. Pap. Geol. Soc Am.*, *404*, 129–138.

Jex, C. N., A. Baker, I. J. Fairchild, W. J. Eastwood, M. J. Leng, H. J. Sloane, L. Thomas, and E. Bekaroglu (2010), Calibration of speleothem $\delta^{18}O$ with instrumental climate records from Turkey, *Global Planet. Change*, *71*(3–4), 207–217, doi:10.1016/j.gloplacha.2009.08.004.

Jocson, J. M. U., J. W. Jenson, and D. N. Contractor (2002), Recharge and aquifer response: Northern Guam Lens Aquifer, Guam, Mariana Islands, *J. Hydrol.*, *260*(1–4), 231–254, doi:10.1016/S0022-1694(01)00617-5.

Johnson, K. R., C. Y. Hu, N. S. Belshaw, and G. M. Henderson (2006), Seasonal trace-element and stable-isotope variations in a Chinese speleothem: The potential for high-resolution paleomonsoon reconstruction, *Earth Planet. Sci. Lett.*, *244*(1–2), 394–407, doi:10.1016/j.epsl.2006.01.064.

Jones, I. C., and J. L. Banner (2003), Estimating recharge thresholds in tropical karst island aquifers: Barbados, Puerto Rico and Guam, *J. Hydrol.*, *278*(1–4), 131–143, doi:10.1016/S0022-1694(03)00138-0.

Juillet-Leclerc, A., S. Thiria, P. Naveau, T. Delcroix, N. Le Bec, D. Blamart, and T. Correge (2006), SPCZ migration and ENSO events during the 20th century as revealed by climate proxies from a Fiji coral, *Geophys. Res. Lett.*, *33*, L17710, doi:10.1029/2006GL025950.

Lachniet, M. S. (2009), Climatic and environmental controls on speleothem oxygen-isotope values, *Quat. Sci. Rev.*, *28*(5–6), 412–432, doi:10.1016/j.quascirev.2008.10.021.

Lorrey, A., P. Williams, J. Salinger, T. Martin, J. Palmer, A. Fowler, J. X. Zhao, and H. Neil (2008), Speleothem stable isotope records interpreted within a multi-proxy framework and implications for New Zealand palaeoclimate reconstruction, *Quat. Int.*, *187*, 52–75.

Mantua, N. J., S. R. Hare, Y. Zhang, J. M. Wallace, and R. C. Francis (1997), A Pacific interdecadal climate oscillation with impacts on salmon production, *Bull. Am. Meteorol. Soc.*, *78*(6), 1069–1079, doi:10.1175/1520-0477(1997)078<1069:APICOW>2.0.CO;2.

Mattey, D., D. Lowry, J. Duffet, R. Fisher, E. Hodge, and S. Frisia (2008), A 53 year seasonally resolved oxygen and carbon isotope record from a modem Gibraltar speleothem: Reconstructed drip water and relationship to local precipitation, *Earth Planet. Sci. Lett.*, *269*(1–2), 80–95, doi:10.1016/j.epsl.2008.01.051.

Mickler, P. J., J. L. Banner, L. Stern, Y. Asmerom, R. L. Edwards, and E. Ito (2004), Stable isotope variations in modern tropical speleothems: Evaluating equilibrium vs. kinetic isotope effects, *Geochim. Cosmochim. Acta*, *68*(21), 4381–4393, doi:10.1016/j.gca.2004.02.012.

Mickler, P. J., L. A. Stern, and J. L. Banner (2006), Large kinetic isotope effects in modern speleothems, *Geol. Soc. Am. Bull.*, *118*(1–2), 65–81, doi:10.1130/B25698.1.

Musgrove, M., J. L. Banner, L. E. Mack, D. M. Combs, E. W. James, H. Cheng, and R. L. Edwards (2001), Geochronology of late Pleistocene to Holocene speleothems from central Texas: Implications for regional paleoclimate, *Geol. Soc. Am. Bull.*, *113*(12), 1532–1543, doi:10.1130/0016-7606(2001)113<1532:GOLPTH>2.0.CO;2.

Partin, J. W., K. M. Cobb, J. F. Adkins, B. Clark, and D. P. Fernandez (2007), Millennial-scale trends in Warm

Pool hydrology since the Last Glacial Maximum, *Nature*, *449*(7161), 452–455, doi:10.1038/nature06164.

Quinn, T. M., F. W. Taylor, and T. J. Crowley (1993), A 173 year stable-isotope record from a tropical South-Pacific coral, *Quat. Sci. Rev.*, *12*(6), 407–418, doi:10.1016/S0277-3791(05)80005-8.

Quinn, T. M., F. W. Taylor, and T. J. Crowley (2006), Coral-based climate variability in the Western Pacific Warm Pool since 1867, *J. Geophys. Res.*, *111*, C11006, doi:10.1029/2005JC003243.

Rasmusson, E. M., and J. M. Wallace (1983), Meteorological aspects of the El Niño–Southern Oscillation, *Science*, *222*(4629), 1195–1202, doi:10.1126/science.222.4629.1195.

Roberts, M. S., P. L. Smart, and A. Baker (1998), Annual trace element variations in a Holocene speleothem, *Earth Planet. Sci. Lett.*, *154*(1–4), 237–246, doi:10.1016/S0012-821X(97)00116-7.

Ropelewski, C. F., and M. S. Halpert (1987), Global and regional scale precipitation patterns associated with the El Niño–Southern Oscillation, *Mon. Weather Rev.*, *115*(8), 1606–1626, doi:10.1175/1520-0493(1987)115<1606:GARSPP>2.0.CO;2.

Rosenthal, Y., D. W. Oppo, and B. K. Linsley (2003), The amplitude and phasing of climate change during the last deglaciation in the Sulu Sea, western equatorial Pacific, *Geophys. Res. Lett.*, *30*(8), 1428, doi:10.1029/2002GL016612.

Rozanski, K., L. Araguas-Araguas, and R. Gonfiantini (1993), Isotopic patterns in modern global precipitation, in *Climate Change in Continental Isotopic Records*, *Geophys. Monogr. Ser.*, vol. 78, edited by P. K. Swart et al., pp. 1–36, AGU, Washington, D. C.

Schimpf, D., R. Kilian, A. Kronz, K. Simon, C. Spotl, G. Worner, M. Deininger, and A. Mangini (2011), The significance of chemical, isotopic, and detrital components in three coeval stalagmites from the superhumid southernmost Andes (53°S) as high-resolution palaeo-climate proxies, *Quat. Sci. Rev.*, *30*(3–4), 443–459, doi:10.1016/j.quascirev.2010.12.006.

Smart, P. L., and H. Friederich (1986), Water movement and storage in the unsaturated zone of a maturely karstified aquifer, Mendip Hills, England, paper presented at the Conference on Environmental Problems in Karst Terrains and Their Solutions, Natl. Water Wells Assoc., Bowling Green, Ky.

Smith, C. L., I. J. Fairchild, C. Spotl, S. Frisia, A. Borsato, S. G. Moreton, and P. M. Wynn (2009), Chronology building using objective identification of annual signals in trace element profiles of stalagmites, *Quat. Geochronol.*, *4*(1), 11–21, doi:10.1016/j.quageo.2008.06.005.

Spotl, C., I. J. Fairchild, and A. F. Tooth (2005), Cave air control on dripwater geochemistry, Obir Caves (Austria):

Implications for speleothem deposition in dynamically ventilated caves, *Geochim. Cosmochim. Acta*, *69*(10), 2451–2468, doi:10.1016/j.gca.2004.12.009.

Stott, L., C. Poulsen, S. Lund, and R. Thunell (2002), Super ENSO and global climate oscillations at millennial time scales, *Science*, *297*(5579), 222–226, doi:10.1126/science.1071627.

Taboroši, D., J. W. Jenson, and J. E. Mylroie (2003), Zones of enhanced dissolution and associated cave morphology in an uplifted carbonate island karst aquifer, northern Guam, Mariana Islands, *Speleogenesis Evol. Karst Aquifers*, *1*(4), 1–16.

Timmermann, A., J. Oberhuber, A. Bacher, M. Esch, M. Latif, and E. Roeckner (1999), Increased El Niño frequency in a climate model forced by future greenhouse warming, *Nature*, *398*(6729), 694–697, doi:10.1038/19505.

Treble, P., J. M. G. Shelley, and J. Chappell (2003), Comparison of high resolution sub-annual records of trace elements in a modern (1911–1992) speleothem with instrumental climate data from southwest Australia, *Earth Planet. Sci. Lett.*, *216*(1–2), 141–153, doi:10.1016/S0012-821X(03)00504-1.

Treble, P. C., J. Chappell, M. K. Gagan, K. D. McKeegan, and T. M. Harrison (2005a), In situ measurement of seasonal δ^{18}O variations and analysis of isotopic trends in a modem speleothem from southwest Australia, *Earth Planet. Sci. Lett.*, *233*(1–2), 17–32, doi:10.1016/j.epsl.2005.02.013.

Treble, P. C., J. Chappell, and J. M. G. Shelley (2005b), Complex speleothem growth processes revealed by trace element mapping and scanning electron microscopy of annual layers, *Geochim. Cosmochim. Acta*, *69*(20), 4855–4863, doi:10.1016/j.gca.2005.06.008.

Vacher, H. L., and J. E. Mylroie (2002), Eogenetic karst from the perspective of an equivalent porous medium, *Carbonates Evaporites*, *17*(2), 182–196, doi:10.1007/BF03176484.

van Breukelen, M. R., H. B. Vonhof, J. C. Hellstrom, W. C. G. Wester, and D. Kroon (2008), Fossil dripwater in stalagmites reveals Holocene temperature and rainfall variation in Amazonia, *Earth Planet. Sci. Lett.*, *275*(1–2), 54–60, doi:10.1016/j.epsl.2008.07.060.

Westaway, K. E., J. X. Zhao, R. G. Roberts, A. R. Chivas, M. J. Morwood, and T. Sutikna (2007), Initial speleothem results from western Flores and eastern Java, Indonesia: Were climate changes from 47 to 5 ka responsible for the extinction of Homo floresiensis?, *J. Quat. Sci.*, *22*(5), 429–438, doi:10.1002/jqs.1122.

Zhang, Y., J. M. Wallace, and D. S. Battisti (1997), ENSO-like interdecadal variability: 1900–93, *J. Clim.*, *10*(5), 1004–1020, doi:10.1175/1520-0442(1997)010<1004:ELIV>2.0.CO;2.